# Geoelectrical inference of mass transfer parameters using temporal moments

Frederick D. Day-Lewis[1] and Kamini Singha[2]

Received 19 December 2007; revised 3 March 2008; accepted 17 March 2008; published 2 May 2008.

[1] We present an approach to infer mass transfer parameters based on (1) an analytical model that relates the temporal moments of mobile and bulk concentration and (2) a bicontinuum modification to Archie's law. Whereas conventional geochemical measurements preferentially sample from the mobile domain, electrical resistivity tomography (ERT) is sensitive to bulk electrical conductivity and, thus, electrolytic solute in both the mobile and immobile domains. We demonstrate the new approach, in which temporal moments of collocated mobile domain conductivity (i.e., conventional sampling) and ERT-estimated bulk conductivity are used to calculate heterogeneous mass transfer rate and immobile porosity fractions in a series of numerical column experiments.

**Citation:** Day-Lewis, F. D., and K. Singha (2008), Geoelectrical inference of mass transfer parameters using temporal moments, *Water Resour. Res.*, *44*, W05201, doi:10.1029/2007WR006750.

## 1. Introduction

[2] Understanding the rates, scaling behavior, and heterogeneity of mass transfer is critical to the reliable prediction of contaminant transport and design of aquifer remediation schemes. Complex concentration tailing and rebound in fractured and heterogeneous porous media have been explained by mass transfer [e.g., *Haggerty and Gorelick*, 1994; *Harvey et al.*, 1994; *Haggerty and Gorelick*, 1995; *Benson et al.*, 2000; *Feehley et al.*, 2000; *Harvey and Gorelick*, 2000; *Dentz and Berkowitz*, 2003]. In models of mass transfer, an aquifer is conceptualized as consisting of multiple, overlapping continua. In the simplest formulation, a representative elementary volume is a bicontinuum consisting of (1) a mobile domain, in which advection and dispersion occur, and (2) an immobile domain, in which diffusion dominates. For the case without sorption,

$$\theta_m \frac{\partial c_m}{\partial t} + \theta_{im} \frac{\partial c_{im}}{\partial t} = \nabla \cdot (\theta_m D \nabla c_m) - \theta_m v \cdot \nabla c_m \qquad (1a)$$

$$\frac{\partial c_{im}}{\partial t} = \alpha (c_m - c_{im}), \qquad (1b)$$

where $c_m$ is the mobile domain concentration [M/L$^3$], $c_{im}$ is the immobile domain concentration [M/L$^3$], $D$ is the hydrodynamic dispersion tensor [L$^2$/T], $v$ is the pore water velocity [L/T], $\theta_m$ is the mobile domain porosity [−], $\theta_{im}$ is the immobile domain porosity [−], $\alpha$ is the mass transfer rate coefficient [T$^{-1}$], and $t$ is time [T]. Solute transfers between domains according to (1b), residing in the immobile domain for an average period of $1/\alpha$; hence mass transfer produces breakthrough curves with long tails compared to standard advective-dispersive transport. Although linear exchange (1b) is commonly assumed, more complicated multirate models exist [*Haggerty and Gorelick*, 1995; *Berkowitz et al.*, 2006]. Mass transfer is thought to occur at the microscopic (e.g., grains), mesoscopic (e.g., fractures), and macroscopic (e.g., hydrofacies) scales [*Haggerty and Gorelick*, 1994; *Feehley et al.*, 2000; *Harvey and Gorelick*, 2000].

[3] Experimental verification and measurement of the parameters controlling mass transfer (i.e., $\alpha$ and $\theta_{im}$) is difficult because conventional sampling draws fluid from the mobile domain and provides only indirect information about the concentration in the immobile domain. Even with extensive coring, it is not possible to sample all scales of heterogeneity in a system, and insight into immobile solute and transfer rates remains problematic. For these reasons, the prevalence of mass transfer remains an issue of debate [*Hill et al.*, 2006; *Molz et al.*, 2006].

[4] Recently, *Singha et al.* [2007] presented experimental data and numerical results indicating that mass transfer has an observable geoelectrical signature. Geoelectrical measurements are sensitive to total concentration of ionic species, rather than just mobile concentration. Experimental data collected during a push-pull freshwater injection into a brackish aquifer showed a hysteretic relation between collocated measurements of bulk and fluid conductivity; these findings are inconsistent with standard advective-dispersive behavior and petrophysical theory [*Archie*, 1942] but were explained by transport models that consider mass transfer. *Singha et al.* [2007] qualitatively reproduced their field-experimental data using first-order, linear mass transfer, and a modified version of Archie's law in which both mobile and immobile porosity contribute to electrolytic conduction. Here, we capitalize on this finding and past work relating the temporal moments of mobile and immobile concentration [*Harvey and Gorelick*, 1995] to calculate mass transfer parameters

[1] U.S. Geological Survey, Storrs, Connecticut, USA.
[2] Department of Geosciences, Pennsylvania State University, University Park, Pennsylvania, USA.


0043-1397/08/2007WR006750

using geoelectrical measurements and conventional fluid sampling.

## 2. Approach

[5] Conventional approaches to estimate mass transfer parameters involve calibration of analytical or numerical models using observations of mobile domain concentrations at the laboratory scale [e.g., *Hollenbeck et al.*, 1999] or field scale [e.g., *Harvey et al.*, 1994; *Feehley et al.*, 2000]. Access to either total or immobile concentration would provide additional information for calibration. *Harvey and Gorelick* [1995] developed algebraic relations between the temporal moments of mobile and immobile domain concentration breakthrough curves. For certain boundary conditions, differences between the temporal moments of $c_m$ and $c_{im}$ are functions solely of $\alpha$, $\theta_m$, and $\theta_{im}$, and are independent of heterogeneity. In the following sections, we present the petrophysical basis for geoelectrical monitoring of mass transfer and inference of heterogeneous mass transfer parameters.

### 2.1. Basis for the Geoelectrical Signature of Mass Transfer

[6] Electrical resistivity tomography (ERT) increasingly is used to monitor hydrologic processes such as transport of conductive tracers in the laboratory [e.g., *Binley et al.*, 1996; *Slater et al.*, 2002] and field [e.g., *Kemna et al.*, 2002; *Singha and Gorelick*, 2005, 2006]. The basis for such work is the sensitivity of bulk conductivity to pore fluid conductivity, as described by Archie's law [*Archie*, 1942]:

$$\sigma_b = a\sigma_f \theta_t^q, \tag{2}$$

where $\sigma_b$ is bulk conductivity [S/m]; $\sigma_f$ is fluid conductivity [S/m]; $\theta_t$ is total porosity [−], the sum of mobile and immobile porosity; $q$ is cementation exponent [−]; and $a$ is a fitting parameter, which is a function of tortuosity. Equation (2) is widely used to relate pore fluid and bulk conductivity in the absence of surface conduction. Although surface conductance is neglected here, it can be addressed with an additional term [e.g., *Worthington*, 1985]. For a bicontinuum, the measured fluid conductivity is that of the mobile domain, and thus collocated measurements of bulk and fluid conductivity may depart from Archie's law depending on mass transfer. Assuming that electrolytic conduction occurs in both domains, we use a modified petrophysical model for the bicontinuum [after *Singha et al.*, 2007]:

$$\sigma_b = a(\theta_m + \theta_{im})^{q-1}\left(\theta_m \sigma_{f,m} + \theta_{im}\sigma_{f,im}\right), \tag{3}$$

where $\sigma_{f,m}$ is the mobile conductivity [S/m], and $\sigma_{f,im}$ is the immobile conductivity [S/m]. We assume here that (1) the fitting parameter $a$ is an effective value for the bicontinuum and (2) bulk electrical conductivity varies linearly with total concentration [e.g., *Keller and Frischknecht*, 1966], and thus the conductivity of mobile and immobile porosities average arithmetically, i.e., as resistors in parallel. This petrophysical model could be adapted for situations where (1) either geometric or harmonic averaging is required or (2) the tortuosities of mobile and immobile domains are known independently.

[7] In ERT, an electrical gradient is established between two source electrodes, and voltages are measured between pairs of receiver electrodes. This procedure is repeated for many four-electrode combinations. Typical ERT data sets comprise hundreds or thousands of measurements. Modern multichannel instruments are capable of collecting multiple potential measurements simultaneously, allowing for rapid data acquisition (i.e., thousands of data per hour).

[8] We simulate ERT data for column experiments using the EIDORS finite element codes [*Adler and Lionheart*, 2006], which permit use of an irregular mesh of tetrahedral elements to accurately represent the column's cylindrical boundary. The ERT inverse problem involves minimization of an objective function combining two terms: (1) the least squares, weighted misfit between observed and predicted measurements and (2) a measure of solution complexity based on a second-derivative spatial filter. The terms are weighted to achieve consistency between simulated and observed measurement errors, i.e., Occam's inversion [*Constable et al.*, 1987].

### 2.2. Inference of Mass Transfer Parameters

[9] Temporal moments are commonly used to describe breakthrough curves. The zeroth- through second-order moments are related to total mass, mean arrival time, and spread, respectively, and are commonly used to infer the rates of decay, advection and dispersion. Higher-order moments are required to describe yet more complicated breakthrough (i.e., skewed or multipeak). The $n$th temporal moment, $m_n$, is defined as

$$m_n = \int_0^\infty t^n c(t) dt, \tag{4}$$

where $c(t)$ is concentration at time $t$ [e.g., *Goltz and Roberts*, 1987].

[10] *Harvey and Gorelick* [1995] derived temporal moment-generating equations for linear and diffusive models of mass transfer under steady state flow conditions. For certain boundary conditions, the temporal moments of $c_m$ and $c_{im}$ at a given location are related by simple algebraic expressions. For example, under linear mass transfer (1b):

$$m_n^{im} = n! \sum_{i=0}^{n} \frac{m_i^m}{i!} \frac{1}{\alpha^{n-i}} + n! \frac{c_{im}^0}{\alpha^n}, \tag{5}$$

where, $c_{im}^0$ is the initial immobile concentration at the observation location; and $m_n^m$, $m_n^{im}$ are the $n$th-order temporal moments of mobile and immobile concentration, respectively. From (5), it is evident that given temporal moments of collocated mobile and immobile concentration, it is possible to calculate mass transfer rate coefficient and porosity fractions. For example, the mean arrival time of immobile concentration is offset from that of mobile concentration by a constant, which is a function of $\alpha$, and this offset is independent of heterogeneity (in $\alpha$ or permeability).

[11] Standard geochemical sampling cannot measure $c_{im}$, so we instead focus on total concentration (solute mass

**Table 1.** Setup for Synthetic Column Experiments

| Parameter | Value |
|---|---|
| Specific discharge | 0.1 m/d |
| Head gradient | 0.01 |
| Hydraulic conductivity, K | 10 m/d |
| Initial concentration, $S_0$ | 1000 mg/L |
| Injection concentration | 100 mg/L |
| $\theta_m$, $\theta_{im}$ | 0.1, 0.25 |
| Cross-sectional diameter | 10 cm |
| Column length | 100 cm |
| Archie a, q | 1, 1 |
| Rate constant, $\alpha$, for homogeneous columns | 0.95, 0.286, 0.095 $d^{-1}$ |
| Rate constant, $\alpha$, for heterogeneous column | 0.8, 0.4, 0.28 $d^{-1}$ |

divided by bulk volume), which for electrolytes can be inferred using geoelectrical methods. Combining the definition of total concentration and (5),

$$m_n^T = \frac{1}{\theta_m + \theta_{im}} \left( \theta_m m_n^m + \theta_{im} n! \sum_{i=0}^{n} \frac{m_i^m}{i!} \frac{1}{\alpha^{n-i}} + n! \frac{S_0}{\alpha^n} \right), \quad (6)$$

where $m_n^T$ is the $n$th temporal moment of total concentration. Consequently, given temporal moments of collocated mobile and total concentration, we can estimate $\alpha$ and porosity fractions for various initial conditions, $S_0$.

[12] For purge experiments, in which immobile and mobile concentration are initially in equilibrium, consideration of temporal moments up to order one produces sufficient nonredundant equations to solve for mass transfer parameters:

$$\alpha = \frac{m_0^T - m_0^m}{m_1^T - m_1^m - m_0^m \left( m_0^T - m_0^m \right) / S_0} \quad (7)$$

$$\frac{\theta_{im}}{\theta_{im} + \theta_m} = \frac{\left( m_0^T - m_0^m \right)^2}{S_0 \left( m_1^T - m_1^m \right) - m_0^m \left( m_0^T - m_0^m \right)} \quad (8)$$

$$\frac{\theta_m}{\theta_{im} + \theta_m} = 1 - \frac{\left( m_0^T - m_0^m \right)^2}{S_0 \left( m_1^T - m_1^m \right) - m_0^m \left( m_0^T - m_0^m \right)}. \quad (9)$$

[13] For an invading solution with nonzero concentration, moments would be calculated on the basis of differences between the injected and background concentrations. Pulse injections of tracer could also be considered; however, moments up to order two are required for the case of zero initial immobile concentration, and calculation of higher-order moments is more prone to error and the limits of ERT resolution than that of lower-order moments. Here, we focus on purge tests, although extension to pulse injections is trivial.

[14] Equations (7)–(9) constitute a framework in which to calculate mass transfer parameters from the temporal moments of mobile domain concentration (i.e., from sampling) and total concentration or surrogate geoelectrical measurements. The procedure is straightforward and does not require inverse modeling. We note, however, that (1) these calculations are based on simple boundary conditions and assume steady state flow; (2) reliable inference of temporal moments can prove difficult with sharp peaks; and (or) strong tailing behavior with truncated breakthrough curves; and (3) the resolving power of geophysical tomography is limited by acquisition geometry, regularization, and measurement error [*Day-Lewis and Lane*, 2004; *Day-Lewis et al.*, 2005, 2007].

## 3. Numerical Examples

[15] We use numerical laboratory-scale column experiments to demonstrate geoelectrical inference of mass transfer parameters and to evaluate the limitations of the approach. Technology for ERT in columns is well established [e.g., *Binley et al.*, 1996]. As discussed in section 2.2, we use the EIDORS toolbox [*Adler and Lionheart*, 2006] to simulate 3-D ERT data and use our own ERT inverse code, which is based on Occam's inversion and smoothness-based regularization. MT3DMS [*Zheng and Wang*, 1999] is used to simulate solute transport with first-order mass transfer. We note that different conventions are used for the mass transfer coefficient, $\alpha$. As formulated in (1), $\alpha$ is equivalent to the inverse of residence time in the immobile domain, whereas in MT3DMS, $\alpha$ is equivalent to immobile porosity divided by immobile residence time; hence values reported here were multiplied by $\theta_{\text{im}}$ for input to MT3DMS.

[16] The experimental design for the column apparatus is summarized in Table 1. For simplicity, transport through the column is assumed to be one dimensional, dispersion is neglected, flow is driven by an imposed head difference across the column, and hydraulic conductivity is homogeneous. The finite difference grid for flow and transport consists of 1-cm cells. A constant concentration boundary condition for the mobile domain is used at the input end of the column to simulate invasion into the mobile domain. The discharge boundary is modeled as an advective flux condition. Prior to the purge experiment, the mobile and immobile domains are in equilibrium.

[17] For the ERT apparatus, we assume a total of 24 electrodes arranged in two rows of 12, with rows parallel to the column axis and 180° apart (Figures 1a and 1b). Electrodes are modeled as 0.5-cm square pads consisting of multiple elements. The finite element mesh comprises 18,420 tetrahedral elements. Current injections involve only 12 electrodes on one side of the column, in skip-1 configurations as described by *Slater et al.* [2000]. For a given current pair, voltages are measured for all remaining electrode pairs for which (1) geometric factors are less than 250 and (2) numerically calculated geometric factors differ by less than 1% between simulations using different homogeneous conductivity fields; these criteria eliminate data for which model noise is large relative to simulated voltages. The resulting acquisition geometry consists of 1573 measurements for each time-lapse data set, which would take perhaps 30–60 min to collect given current technology. Simulated ERT data sets are collected at 3-h intervals for 25 d. Gaussian errors with zero mean and 1.5% standard deviation are added to the simulated data and used also for weighting measurements in the inversion. The average pore fluid velocity (1 m/d) is slow relative to data collection; hence temporal smearing should be negligible. Inversion parameters correspond to patches of elements in 5-cm intervals along the column.

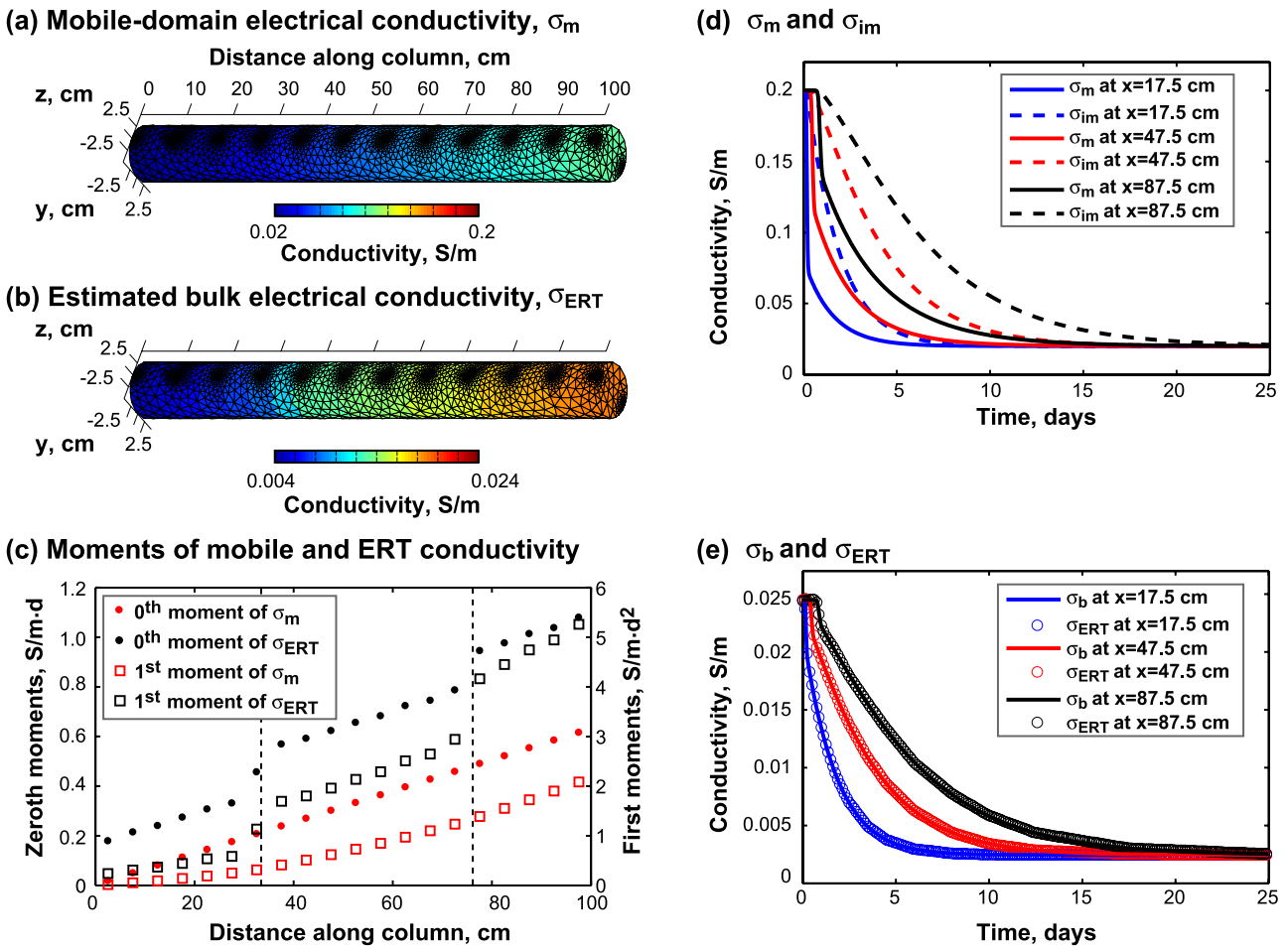


**Figure 1.** For the heterogeneous column (a) mobile domain fluid conductivity within the finite element mesh at 2.5 d after start of injection, (b) estimated bulk electrical conductivity from electrical resistivity tomography (ERT) at 2.5 d, (c) temporal moments of mobile domain fluid conductivity and estimated bulk electrical conductivity, (d) breakthrough curves of mobile domain and immobile domain fluid conductivity at three locations, and (e) estimated and true bulk conductivity at three locations. Dashed lines in Figure 1c indicate zonation for heterogeneous rate constant.

[18] We consider numerical examples for scenarios involving (1) homogeneous $\alpha$, over a range from 0.1 to 1 $d^{-1}$ and (2) zonal heterogeneity of $\alpha$. For the purpose of illustration, we assume fluid sampling can occur anywhere in the column, although in practice only a few ports or probes would be used or required. Temporal moments are calculated for time series of ERT-estimated bulk conductivity and sampled fluid conductivity at 10-cm intervals along the column (e.g., Figures 1c, 1d, and 1e), and $\alpha$ and $\theta_{im}/\theta_t$ are calculated using (7)–(8), after differencing both series to account for the conductivity of the injectate and normalizing the ERT estimates by the ratio of the initial mobile to initial bulk conductivity. The results for homogeneous (Figure 2a) and heterogeneous columns (Figure 2b) indicate that our approach produces accurate estimates of mass transfer parameters for about an order-of-magnitude range in $\alpha$. For this example, $\alpha$ above approximately 1.0 $d^{-1}$ results in exchange between domains so rapid that the breakthrough curves for $c_m$ and $c_{im}$ are near equilibrium and the calculated first moments are unreliable. Conversely, for $\alpha$ below approximately 0.1 $d^{-1}$, the exchange between domains is so slow that the immobile domain is not purged effectively during the 25-d experiment, resulting in truncated breakthrough curves and spurious estimates of temporal moments. Truncation results in overestimates of $\alpha$ (Figure 2a), with the bias worst toward the discharge end of the column, which is purged last and least effectively. These insights into experiment design and limitations can be explained and predicted using the Damkohler number, *DaI*, a dimensionless measure of the effect of mass transfer relative to advection [e.g., *Bahr and Rubin*, 1987]:

$$DaI = \frac{\alpha(1+\theta_{im}/\theta_m)L}{v}, \tag{10}$$

where $L$ is the domain length. For the assumed experimental setup, the approach is effective for $0.333 < DaI < 3.33$ (Figure 2a). We stress that the limitations discussed can be addressed by experiment design (i.e., column length, experiment duration, discharge rate) to achieve favorable *DaI* given the material under study; furthermore, these limitations are not specific to our framework but also impact

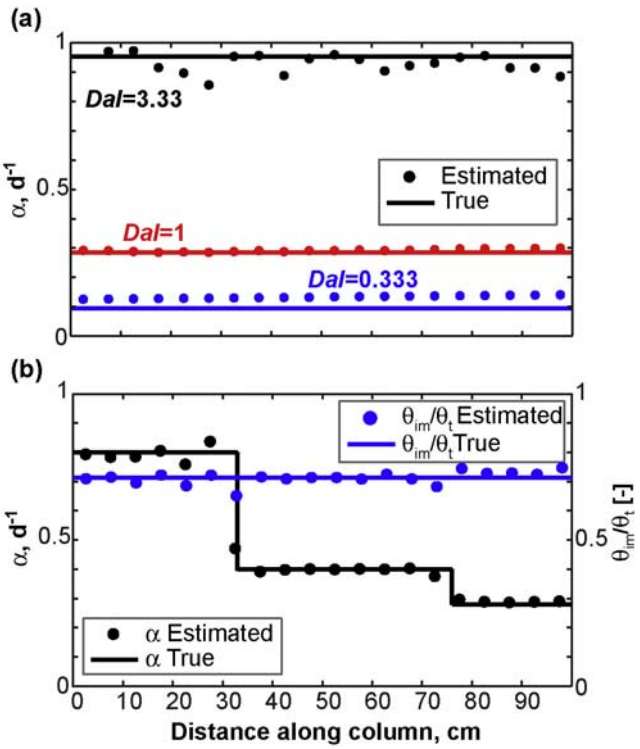


**Figure 2.** (a) Estimated and true rate coefficient, $\alpha$, for three homogeneous columns with Damkohler numbers, *DaI*, of 0.333, 1, and 3.33 and (b) estimated and true rate coefficient and immobile porosity fraction for the heterogeneous column.

conventional measurement of mass transfer [e.g., *Wagner and Harvey*, 1997; *Wörman and Wachniew*, 2007].

## 4. Discussion and Conclusions

[19] New approaches are required for experimental verification and measurement of heterogeneous mass transfer parameters. Recent work suggests that mass transfer manifests an observable geoelectrical signature, and that geoelectrical monitoring of tracer tests can provide insight into mass transfer. We presented a framework in which to calculate heterogeneous mass transfer rate coefficients and porosity fractions on the basis of the temporal moments of collocated (1) fluid electrical conductivity and (2) bulk electrical conductivity from ERT. Numerical experiments for laboratory-scale columns demonstrated the approach's potential, as well as its limitations. A given experimental design provides robust estimates over only a finite range of rate coefficient. We used the experimental Damkohler number, *DaI*, to bound the utility of our approach and provide guidelines for experiment design. We achieved good results for $0.333 < DaI < 3.33$. For experiments with greater *DaI*, the mobile and immobile domains are in approximate local equilibrium, with negligible separation between breakthrough curves. For lower *DaI*, the immobile domain is not purged during the experiment, leading to truncated breakthrough curves and biased estimates. The column length, discharge rate, and experiment duration must, therefore, be selected in combination and with consideration of the material under study; moreover, the ERT acquisition must be sufficiently rapid to resolve breakthrough.

[20] Although this study focused on column-scale numerical experiments, our results have clear implications for improved characterization of parameters that control field-scale transport in aquifer and fluvial systems, where mass transfer limits the efficiency of aquifer storage and recovery [*Culkin et al.*, 2008] and remediation [*Haggerty and Gorelick*, 1994] activities. ERT can provide time-lapse information over a broad range of spatial scales, and our approach could be adapted for analysis of field-scale tracer tests or extended through (1) inverse modeling to consider more complicated, multirate models of mass transfer or (2) incorporation of approaches to improve moment inference and address truncated breakthrough curves [e.g., *Jose and Cirpka*, 2004; *Wörman and Wachniew*, 2007].

[21] **Acknowledgments.** This work was funded by the U.S. Geological Survey Toxic Substances Hydrology and Ground-Water Resources Programs and American Chemical Society PRF grant 45206-G8 to K.S. The authors are grateful to John W. Lane Jr. and Rory Henderson (USGS) for comments on this work and to Lee Slater, Olaf Cirpka, and an anonymous reviewer for useful suggestions and comments on the draft manuscript.

## References

Adler, A., and W. R. B. Lionheart (2006), Uses and abuses of EIDORS: An extensible software base for EIT, *Physiol. Meas.*, *27*, S25–S42, doi:10.1088/0967-3334/27/5/S03.

Archie, G. E. (1942), The electrical resistivity log as an aid in determining some reservoir characteristics, *Trans. Am. Inst. Min. Metall. Pet. Eng.*, *146*, 54–62.

Bahr, J. M., and J. Rubin (1987), Direct comparison of kinetic and local equilibrium formulations for solute transport affected by surface reactions, *Water Resour. Res.*, *23*(3), 438–452, doi:10.1029/WR023i003p00438.

Benson, D. A., S. W. Wheatcraft, and M. M. Meerschaert (2000), Application of a fractional advection-dispersion equation, *Water Resour. Res.*, *36*(6), 1403–1412, doi:10.1029/2000WR900031.

Berkowitz, B., A. Cortis, M. Dentz, and H. Scher (2006), Modeling non-Fickian transport in geological formations as a continuous time random walk, *Rev. Geophys.*, *44*, RG2003, doi:10.1029/2005RG000178.

Binley, A., S. Henry-Poulter, and B. Shaw (1996), Examination of solute transport in an undisturbed soil column using electrical resistance tomography, *Water Resour. Res.*, *32*(4), 763–769, doi:10.1029/95WR02995.

Constable, S. C., R. L. Parker, and C. G. Constable (1987), Occam's inversion: A practical algorithm for generating smooth models from electromagnetic sounding data, *Geophysics*, *52*, 289–300, doi:10.1190/1.1442303.

Culkin, S. L., K. Singha, and F. D. Day-Lewis (2008), Implications of rate-limited mass transfer for aquifer storage and recovery, *Groundwater*, doi:10.1111/j.1745-6584.2008.00435.X, in press.

Day-Lewis, F. D., and J. W. Lane Jr. (2004), Assessing the resolution-dependent utility of tomograms for geostatistics, *Geophys. Res. Lett.*, *31*, L07503, doi:10.1029/2004GL019617.

Day-Lewis, F. D., K. Singha, and A. M. Binley (2005), Applying petrophysical models to radar travel time and electrical resistivity tomograms: Resolution-dependent limitations, *J. Geophys. Res.*, *110*, B08206, doi:10.1029/2004JB003569.

Day-Lewis, F. D., Y. Chen, and K. Singha (2007), Moment inference from tomograms, *Geophys. Res. Lett.*, *34*, L22404, doi:10.1029/2007GL031621.

Dentz, M., and B. Berkowitz (2003), Transport behavior of a passive solute in continuous time random walks and multirate mass transfer, *Water Resour. Res.*, *39*(5), 1111, doi:10.1029/2001WR001163.

Feehley, C. E., C. Zheng, and F. J. Molz (2000), A dual-domain mass transfer approach for modeling solute transport in heterogeneous aquifers: Application to the Macrodispersion Experiment (MADE) site, *Water Resour. Res.*, *36*(9), 2501–2516, doi:10.1029/2000WR900148.

Goltz, M. N., and P. V. Roberts (1987), Using the method of moments to analyze three-dimensional diffusion-limited solute transport from

temporal and spatial perspectives, *Water Resour. Res.*, *23*(8), 1575–1585, doi:10.1029/WR023i008p01575.

Haggerty, R., and S. M. Gorelick (1994), Design of multiple contaminant remediation: Sensitivity to rate-limited mass transfer, *Water Resour. Res.*, *30*(2), 435–446, doi:10.1029/93WR02984.

Haggerty, R., and S. M. Gorelick (1995), Multiple-rate mass transfer for modeling diffusion and surface reactions in media with pore-scale heterogeneity, *Water Resour. Res.*, *31*(10), 2383–2400.

Harvey, C. F., and S. M. Gorelick (1995), Temporal moment-generating equations: Modeling transport and mass transfer in heterogeneous aquifers, *Water Resour. Res.*, *31*(8), 1895–1911, doi:10.1029/95WR01231.

Harvey, C., and S. M. Gorelick (2000), Rate-limited mass transfer or macrodispersion: Which dominates plume evolution at the Macrodispersion Experiment (MADE) site?, *Water Resour. Res.*, *36*(3), 637–650, doi:10.1029/1999WR900247.

Harvey, C. F., R. Haggerty, and S. M. Gorelick (1994), Aquifer remediation: A method for estimating mass transfer rate coefficients and an evaluation of pulsed pumping, *Water Resour. Res.*, *30*(7), 1979–1992, doi:10.1029/94WR00763.

Hill, M. C., H. C. Barlebo, and D. Rosbjerg (2006), Reply to comment by F. Molz et al. on ''Investigating the Macrodispersion Experiment (MADE) site in Columbus, Mississippi, using a three-dimensional inverse flow and transport model,'' *Water Resour. Res.*, *42*, W06604, doi:10.1029/2005WR004624.

Hollenbeck, K. J., C. F. Harvey, R. Haggerty, and C. J. Werth (1999), A method for estimating distributions of mass transfer rate coefficients with application to purging and batch experiments, *J. Contam. Hydrol.*, *37*, 367–388, doi:10.1016/S0169-7722(98)00165-X.

Jose, S. C., and O. A. Cirpka (2004), Measurement of mixing-controlled reactive transport in homogeneous porous media and its prediction from conservative tracer test data, *Environ. Sci. Technol.*, *38*(7), 2089–2096, doi:10.1021/es034586b.

Keller, G. V., and F. C. Frischknecht (1966), *Electrical Methods in Geophysical Prospecting*, 523 pp., Pergamon, Oxford, U.K.

Kemna, A., J. Vanderborght, B. Kulessa, and H. Vereecken (2002), Imaging and characterisation of subsurface solute transport using electrical resistivity tomography (ERT) and equivalent transport models, *J. Hydrol.*, *267*, 125–146, doi:10.1016/S0022-1694(02)00145-2.

Molz, F. J., C. Zheng, S. M. Gorelick, and C. F. Harvey (2006), Comment on ''Investigating the Macrodispersion Experiment (MADE) site in Columbus, Mississippi, using a three-dimensional inverse flow and transport model'' by Heidi Christiansen Barlebo, M.C. Hill, and D. Rosbjerg, *Water Resour. Res.*, *42*, W06603, doi:10.1029/2005WR004265.

Singha, K., and S. M. Gorelick (2005), Saline tracer visualized with three-dimensional electrical resistivity tomography: Field scale moment analysis, *Water Resour. Res.*, *41*, W05023, doi:10.1029/2004WR003460.

Singha, K., and S. M. Gorelick (2006), Effects of spatially variable resolution on field-scale estimates of tracer concentration from electrical inversions using Archie's law, *Geophysics*, *71*(3), G83–G91, doi:10.1190/1.2194900.

Singha, K., F. D. Day-Lewis, and J. W. Lane, Jr. (2007), Geoelectrical evidence for bicontinuum transport in groundwater, *Geophys. Res. Lett.*, *34*, L12401, doi:10.1029/2007GL030019.

Slater, L., A. M. Binley, W. Daily, and R. Johnson (2000), Cross-hole electrical imaging of a controlled saline tracer injection, *J. Appl. Geophys.*, *44*(2–3), 85–102, doi:10.1016/S0926-9851(00)00002-1.

Slater, L., A. Binley, R. Versteeg, G. Cassiani, R. Birken, and S. Sandberg (2002), A 3D ERT study of solute transport in a large experimental tank, *J. Appl. Geophys.*, *49*, 211–229, doi:10.1016/S0926-9851(02)00124-6.

Wagner, B. J., and J. D. Harvey (1997), Experimental design for estimating parameters of rate-limited mass transfer: Analysis of stream tracer studies, *Water Resour. Res.*, *33*(7), 1731–1741, doi:10.1029/97WR01067.

Wörman, A., and P. Wachniew (2007), Reach scale and evaluation methods as limitations for transient storage properties in streams and rivers, *Water Resour. Res.*, *43*, W10405, doi:10.1029/2006WR005808.

Worthington, P. F. (1985), Evolution of shaley sand concepts in reservoir evaluation, *Log Anal.*, *26*, 23–40.

Zheng, C., and P. P. Wang (1999), MT3DMS: A modular three-dimensional multispecies model for simulation of advection, dispersion and chemical reactions of contaminants in groundwater systems: Documentation and user's guide, *Rep. SERDP-99-1*, 202 pp., U.S. Army Eng. Res. and Dev. Cent., Vicksburg, Miss.

F. D. Day-Lewis, Office of Ground Water, Branch of Geophysics, U.S. Geological Survey, 11 Sherman Place, Unit 5015, Storrs, CT 06269, USA. (daylewis@usgs.gov)

K. Singha, Department of Geosciences, Pennsylvania State University, 311 Deike Building, University Park, PA 16802, USA.